



Evaluating the Relationship Between the Carbon and Sulfur Cycles in the Later Cambrian Ocean: An Example from the Port au Port Group, Western Newfoundland, Canada

Citation

Hurtgen, Matthew T., Sara B. Pruss, and Andrew Herbert Knoll. 2009. Evaluating the relationship between the carbon and sulfur cycles in the later Cambrian ocean: An example from the Port au Port Group, western Newfoundland, Canada. *Earth and Planetary Science Letters* 281(3-4): 288-297.

Published Version

doi:10.1016/j.epsl.2009.02.033

Permanent link

<http://nrs.harvard.edu/urn-3:HUL.InstRepos:3988784>

Terms of Use

This article was downloaded from Harvard University's DASH repository, and is made available under the terms and conditions applicable to Open Access Policy Articles, as set forth at <http://nrs.harvard.edu/urn-3:HUL.InstRepos:dash.current.terms-of-use#OAP>

Share Your Story

The Harvard community has made this article openly available.
Please share how this access benefits you. [Submit a story](#).

[Accessibility](#)

Evaluating the relationship between the carbon and sulfur cycles in the later Cambrian ocean: An example from the Port au Port Group, western Newfoundland, Canada

Matthew T. Hurtgen¹

Department of Earth and Planetary Sciences, Northwestern University, Evanston, IL 60208, USA

Sara Pruss

Department of Geology, Smith College, Northampton, Massachusetts 01063, USA

Andrew H. Knoll

Department of Organismic and Evolutionary Biology, Harvard University, Cambridge, Massachusetts 02138, USA

¹ Corresponding author: matt@earth.northwestern.edu, *ph* 847.491.7539, *fax* 847.491.8060

ABSTRACT

We present a high-resolution $\delta^{34}\text{S}$ (sulfate and pyrite) and $\delta^{13}\text{C}_{\text{carbonate}}$ record from the Middle-Upper Cambrian Port au Port Group, a mixed carbonate-siliciclastic succession exposed in western Newfoundland, Canada. The results illustrate systematic $\delta^{34}\text{S}_{\text{sulfate}}$ shifts of $>15\text{‰}$ over relatively short stratigraphic intervals (10 m, likely <1 m.y.), low average $\Delta^{34}\text{S}_{\text{sulfate-pyrite}}$ (ca. 23 ‰) and a generally positive coupling between changes in $\delta^{13}\text{C}_{\text{carbonate}}$ and $\delta^{34}\text{S}_{\text{sulfate}}$. Together, these results indicate that Middle to Late Cambrian sulfate concentrations were low and that the sulfate reservoir was more sensitive to change than it was in either terminal Neoproterozoic or Cenozoic oceans. However, a simple carbon (C) and sulfur (S) isotope box model of the Late Cambrian ocean illustrates that low sulfate concentrations alone fail to account for the $>15\text{‰}$ $\delta^{34}\text{S}_{\text{sulfate}}$ shifts recognized in Port au Port strata. Such large shifts can be generated only if fluctuating oceanic redox is invoked; marine anoxia forces reduced C/S burial and elevated $\Delta^{34}\text{S}$, driving larger $\delta^{34}\text{S}$ changes per mole of organic carbon buried. The conclusion that later Cambrian oceans featured both low sulfate levels and widespread subsurface anoxia supports hypotheses that link fluctuating marine redox conditions in the delayed recovery of skeletal animals and metazoan reefs from late Early Cambrian extinction.

Keywords: Cambrian, sulfate, anoxic, sulfur isotopes, Newfoundland, SPICE

1 **1. Introduction**

2 The biogeochemical cycles of carbon (C) and sulfur (S) are intimately linked through a
3 variety of feedbacks that operate on timescales of days to millions of years. For example, under
4 anaerobic conditions, some bacteria respire organic matter via sulfate reduction, reducing sulfate
5 to sulfide that then reacts with iron (Fe), assuming it is available, to form pyrite. On much
6 longer timescales, increases in organic carbon (OC) burial can drive an increase in atmospheric
7 O₂ concentration which, in turn, facilitates an increase in the extent to which sulfides on land are
8 oxidatively weathered and, ultimately, delivered to the oceans as riverine sulfate. These two
9 processes impose very different relationships between the C isotope composition of dissolved
10 inorganic carbon (DIC) and the sulfur isotope composition of sulfate in seawater. The former
11 leads to a positive correlation between $\delta^{13}\text{C}_{\text{carbonate}}$ (assumed to reflect the $\delta^{13}\text{C}$ of DIC) and
12 $\delta^{34}\text{S}_{\text{sulfate}}$ whereas the latter prescribes a long-term negative correlation (e.g., Veizer et al., 1980).
13 Of course, the recognition of either a positive or negative correlation between $\delta^{13}\text{C}_{\text{carbonate}}$ and
14 $\delta^{34}\text{S}_{\text{sulfate}}$ depends strongly on the relative residence times of seawater DIC and sulfate, neither of
15 which is well constrained for the Cambrian Period.

16 In the modern ocean, the concentration of DIC is ~2 mM with a residence time of ~100
17 k.y. (Bernier and Bernier, 1996). Because of this relatively short residence time, the $\delta^{13}\text{C}$
18 composition of DIC is susceptible to both heterogeneity among the world's ocean basins and
19 short-term (<1 m.y.) change. In contrast, $\delta^{34}\text{S}_{\text{sulfate}}$ is both homogenous throughout the ocean
20 (Rees, 1978) and buffered against short-term variations due to the relatively high concentration
21 (28 mM) and long residence time (~25 m.y.) of sulfate in the oceans (Holser et al. 1989). The
22 large inequality in the residence times of DIC and sulfate in the recent geologic past (i.e., the
23 Cenozoic) has made it difficult to evaluate the relationship between these two biogeochemical

24 cycles that play an important role in regulating Earth's climate (e.g., Kurtz et al., 2003, Paytan et
25 al., 2004).

26 Recent work highlighting the $\delta^{34}\text{S}$ composition of carbonate-associated sulfate (CAS) and
27 pyrite suggests that seawater sulfate concentrations increased near the end of the Neoproterozoic
28 Era (Hurtgen et al., 2005; Fike et al., 2006; Halverson and Hurtgen, 2007). However, the
29 chemical composition of fluid inclusions encased in halite (Horita et al., 2002; Lowenstein et al.,
30 2001, 2003; Brennan et al. 2004; Petrychenko et al., 2005) and the recognition of ^{34}S -enriched
31 CAS (Kampschulte and Strauss, 2004; Gill et al., 2007), pyrite (Strauss, 1999) and francolite-
32 bound sulfate (Hough et al., 2006) in Lower to Middle Cambrian strata indicate that sulfate
33 levels may have been substantially lower during this time interval relative to both the terminal
34 Neoproterozoic and Cenozoic oceans.

35 Here, we present a detailed $\delta^{13}\text{C}_{\text{carbonate}}$ and $\delta^{34}\text{S}$ (sulfate and pyrite) record from the
36 Middle-Upper Cambrian Port au Port Group, western Newfoundland, Canada. These sediments
37 record two intervals marked by C isotope excursions, including a $\sim 4\%$ positive $\delta^{13}\text{C}_{\text{carbonate}}$
38 excursion that has been identified in a number of localities around the world (the SPICE event,
39 Saltzman et al., 2004). Because of this, the Port au Port succession provides an unusual
40 opportunity to explore the relationship between the marine geochemical cycles of C and S during
41 a time interval when the characteristic response times of the DIC and sulfate reservoirs may have
42 been more closely balanced than they are at present. Finally, insights gleaned from the
43 relationship between the C and S cycles during the Cambrian Period may provide an important
44 environmental context for biological changes during this interval, including the 40 m.y. paucity
45 of robust skeletonized fossils in Middle Cambrian through Early Ordovician rocks (e.g., Knoll,
46 2003; Rowland and Shapiro, 2002; Pruss et al., in review).

47

48 **2. Background**

49 *2.1 Geochemical cycles of C and S: Mass balance and isotopic considerations*

50 The $\delta^{13}\text{C}$ and $\delta^{34}\text{S}$ composition of seawater DIC and sulfate, respectively, are dictated by
51 the mass and isotopic compositions of C and S fluxes into and out of the ocean. For C, the
52 primary input is riverine delivery of DIC resulting from the weathering of crustal rocks. C is
53 removed from marine waters through photosynthesis and subsequent OC burial, as well as by
54 carbonate precipitation and deposition. Analogous to the C cycle, the primary input of S (as
55 sulfate) to seawater is riverine delivery resulting from the oxidative weathering of sulfides and
56 dissolution of evaporites (principally calcium sulfates) and carbonates (e.g., CAS) on land.
57 Sulfate is removed from the ocean via evaporite and carbonate deposition, as well as by bacterial
58 sulfate reduction (BSR) and associated pyrite deposition.

59 Balanced changes in the burial of OC and pyrite have played an important role in
60 regulating atmospheric oxygen concentrations through geologic time (Holland, 1973, 1984;
61 Berner and Raiswell, 1983; Kump and Garrels, 1986; Berner 1987). BSR participates in, and so
62 links, the geochemical cycles of C and S. In the presence of oxygen, OC, produced via
63 photosynthesis in the water column, sinks and is respired aerobically. Once oxygen is
64 consumed, either within the water column or sediments, some microbes decompose OC via BSR,
65 reducing sulfate to sulfide that may react with available iron (Fe) to form sedimentary pyrite.
66 Therefore, increased delivery of OC increases oxygen demand, leading to increased BSR, sulfide
67 production and pyrite formation (Berner and Raiswell, 1983).

68 A kinetic isotope effect accompanies the production of both OC and sulfide during
69 photosynthesis and BSR, respectively. The light isotope (i.e., ^{12}C and ^{32}S) is preferentially

70 removed from the terminal electron acceptor (i.e., CO₂ and sulfate) during the production of both
 71 OC and sulfide. Within this context, a global increase in OC production and supply to marine
 72 sediments should result in increased production of pyrite and, therefore, a positive shift in the C
 73 and S isotope compositions of the marine DIC and sulfate reservoirs, respectively. However, as
 74 noted above, the characteristic response times of DIC and sulfate strongly influence the rate and
 75 magnitude at which the isotope composition of each reservoir can shift.

76 Here, reservoir- and time-dependent mass balance equations for $\delta^{13}\text{C}_{\text{carbonate}}$ and $\delta^{34}\text{S}_{\text{sulfate}}$
 77 (adopted from Kump and Arthur, 1999; Kurtz et al., 2003 and Kah et al., 2004) are used to
 78 illustrate how the individual residence times of marine DIC and sulfate influence the degree to
 79 which perturbations to the coupled geochemical cycles of C and S affect the rate and magnitude
 80 of isotopic change. The C isotope composition of carbonate deposition ($\delta^{13}\text{C}_{\text{carbonate}}$) is assumed
 81 to reflect the $\delta^{13}\text{C}$ of the DIC pool from which it precipitated and is represented by:

$$82 \quad \frac{d}{dt} \delta^{13}\text{C}_{\text{carbonate}} = \frac{F_{wc}(\delta_{wc} - \delta^{13}\text{C}_{\text{carbonate}}) - F_{org}\Delta^{13}\text{C}}{M_c} \quad (1)$$

83 where F_{wc} is the total input flux of C to the ocean-atmosphere system from weathering, δ_{wc} is the
 84 isotope composition of that weathering component, F_{org} represents the amount of OC buried,
 85 $\Delta^{13}\text{C}$ represents the average isotope fractionation incurred during the production of OC, and M_c
 86 is the mass of dissolved carbonate in the ocean. Similarly, the S isotope composition of sulfate
 87 deposition ($\delta^{34}\text{S}_{\text{sulfate}}$) is assumed to reflect the $\delta^{34}\text{S}$ of the seawater from which it precipitated
 88 and is represented by:

$$89 \quad \frac{d}{dt} \delta^{34}\text{S}_{\text{sulfate}} = \frac{F_{ws}(\delta_{ws} - \delta^{34}\text{S}_{\text{sulfate}}) - F_{py}\Delta^{34}\text{S}}{M_s} \quad (2)$$

90 where F_{ws} is the total input flux of S to the ocean-atmosphere system from weathering, δ_{ws} is the
91 isotope composition of that weathering component, F_{py} is the total amount of pyrite buried and
92 $\Delta^{34}\text{S}$ is the average net isotope fractionation between seawater sulfate and pyrite resulting from
93 the processes (e.g., BSR, disproportionation of intermediate S species, sulfide oxidation)
94 associated with iron sulfide formation, and M_s is the mass of sulfate in the ocean. Note, sulfate
95 removed from the oceans via calcium sulfate precipitation in evaporite settings involves minimal
96 isotopic fractionation (0-2.4‰; Ault and Kulp, 1959; Raab and Spiro, 1991) and is excluded
97 from this model. However, large-scale changes in evaporite deposition might significantly
98 influence oceanic $\delta^{34}\text{S}_{\text{sulfate}}$.

99 Here, we consider the response of $\delta^{13}\text{C}_{\text{carbonate}}$ and $\delta^{34}\text{S}_{\text{sulfate}}$ to a 50% increase in F_{org} and
100 F_{py} for 1 m.y. (from 2 to 3 m.y. in Fig. 1). Initial conditions were constructed using equations (1)
101 and (2) and mass, fluxes and isotope compositions were adopted from Kurtz et al. (2003) and
102 approximate the Cenozoic C and S cycles at steady state (Table 1). The C and S cycles are
103 linked using a constant C/S burial ratio of 7.7 (Bernier and Raiswell, 1983; Raiswell and Bernier,
104 1985). The 50% increase in F_{org} and F_{py} manifests as a 2.8‰ positive excursion in $\delta^{13}\text{C}$ but a
105 negligible (0.3‰) shift in $\delta^{34}\text{S}_{\text{sulfate}}$. Of course, this is a simplified model of a more complex
106 system, but it illustrates the importance of concentration and residence time when interpreting
107 perturbations to the coupled C and S cycles at various times in Earth history.

108

109 **3. Geologic Setting**

110 *3.1 The Port au Port Group, Newfoundland, Canada*

111 The Middle and Upper Cambrian Port au Port Group is exposed on the south-facing shore
112 of the Port au Port peninsula in western Newfoundland. The succession records Sauk II and

113 Sauk III transgression and was deposited autochthonously on the southeastern margin of
114 equatorial Laurentia in a subtidal-peritidal setting on a mixed carbonate-clastic platform (Chow
115 and James, 1987; Cowan and James, 1993).

116 The basal unit of the Port au Port Group, the March Point Formation (~35 m),
117 disconformably overlies siliciclastic rocks of the Lower Cambrian Hawke Bay Formation.
118 March Point lithologies comprise interbedded glauconitic and phosphatic silicilastics, along
119 with thinly-bedded nodular limestones; they include the deepest water facies preserved in the
120 Middle and Upper Cambrian succession, with some units likely deposited below storm wave
121 base. The overlying Cape Ann Member (~15 m) of the Petit Jardin Formation contains olive-
122 colored shales as well as a few thrombolitic carbonate horizons. The overlying Campbell's
123 Member (~100 m) consists largely of oolites, microbial build-ups, and fine grained carbonate
124 lithologies. The succeeding Big Cove Member, in turn, is a 40-m-thick succession of mostly
125 olive and gray shales with thin limestone beds. The shales are replaced by oolites and microbial
126 build-ups in the overlying Felix Member (50 m). The Man O' War Member (55 m) is
127 lithologically similar to the underlying Felix Member but contains a greater proportion of
128 siliciclastic sediments. Microbial build-ups are common features throughout the March Point
129 and Petit Jardin formations but skeletal limestones are rare.

130 The March Point Formation preserves a *Bolaspidella* trilobite fauna, which indicates an
131 upper Middle Cambrian age. The SPICE event ($>4\text{‰ } \delta^{13}\text{C}_{\text{carbonate}}$ positive excursion) has
132 previously been identified in this particular section by Saltzman et al. (2004) and is
133 biostratigraphically constrained to the *Aphelaspis*, *Dunderbergia*, and *Elvinia* trilobite zones
134 (Cowan and James, 1993; Saltzman et al., 2004), which are Upper Cambrian (Steptoean) in age.
135 Absolute age dates are absent from Port au Port strata, but given these broad biostratigraphic and

136 chemostratigraphic constraints, the section of the Port au Port Group addressed in this study was,
137 in all probability, deposited over 5-10 million years.

138

139 **4. Methods**

140 Carbonate-associated sulfate (CAS) and pyrite were extracted using the techniques of
141 Burdett et al. (1989) and Canfield et al. (1986), respectively. S isotope results are reported as per
142 mil (‰) deviations from the S isotope composition of Vienna Canon Diablo Troilite (VCDT),
143 using the conventional delta ($\delta^{34}\text{S}$) notation; results were generally reproducible to within \pm
144 0.2‰. C isotope ratios are expressed as ‰ deviations relative to VPDB in the standard delta
145 ($\delta^{13}\text{C}$) notation. Average external precision is estimated to be better than 0.1‰. S and C isotope
146 data are provided in Supplementary Tables 1 and 2, respectively.

147

148 **5. Results**

149 Carbonate C isotope values ($\delta^{13}\text{C}$) shift systematically through the section, with values
150 ranging from \sim -4 to 2‰ (Fig. 2). Here, we focus on two intervals marked by sizable C isotope
151 excursions. The first encompasses the March Point Formation and the Cape Ann and lower
152 Campbell's members of the Petit Jardin Formation. $\delta^{13}\text{C}$ increases from a low of \sim -2.5‰ at the
153 base of the section to an average of -0.5‰ over approximately 30 m, drops to -4‰ over the next
154 30 m (in the Cape Ann Member) and then rises again to an average of \sim -0.5‰. $\delta^{34}\text{S}_{\text{sulfate}}$ follows
155 a similar although more exaggerated pattern, with values starting at \sim 30‰, falling to 15‰ and
156 then increasing to values $>$ 40‰ (Fig. 2). The initial drop in $\delta^{34}\text{S}_{\text{sulfate}}$ precedes the decline in
157 $\delta^{13}\text{C}$ by \sim 25 m. $\delta^{34}\text{S}_{\text{pyrite}}$ generally mimics $\delta^{34}\text{S}_{\text{sulfate}}$ through this interval; values begin around

158 15‰, decline to around 0‰ (one value reaches -12‰) before increasing to >25‰. Calculated
159 $\Delta^{34}\text{S}$ ($\delta^{34}\text{S}_{\text{sulfate}} - \delta^{34}\text{S}_{\text{pyrite}}$) values through this interval range from 6 to 24‰.

160 The second interval includes the upper portion of the Big Cove Member, and the Felix
161 and the Man O' War members of the Petit Jardin Formation. $\delta^{13}\text{C}$ begins at -1‰, falls steadily
162 over the next 35 m to -2‰, increases to nearly 2‰ over the next 30 m and then shifts to -3‰
163 over 25 m. This positive excursion, termed the SPICE event, has been recognized in time-
164 equivalent sections globally, although absolute values vary from location to location (e.g.,
165 Saltzman et al., 2000, 2004).

166 In the upper Big Cove Member, $\delta^{34}\text{S}_{\text{sulfate}}$ drops sharply from >40 to 27‰ with virtually
167 no change in $\delta^{13}\text{C}$. Furthermore, $\delta^{34}\text{S}_{\text{sulfate}}$ values do not shift to markedly heavier values through
168 the SPICE event, but do fall at the upper end of the C isotope excursion. The $\delta^{34}\text{S}_{\text{pyrite}}$ record is
169 sparse through this interval (limited pyrite availability) but shows values that range from 0 to
170 9‰. $\Delta^{34}\text{S}$ values begin >40‰ in the upper Big Cove Member and fall to ~20‰ in the Man O'
171 War Member.

172 While negative $\delta^{13}\text{C}_{\text{carbonate}}$ excursions in particular appear to correspond to lithologic
173 transitions in the Port au Port strata, the relationship between these two variables is not
174 systematic. For example, one negative $\delta^{13}\text{C}$ excursion is associated with relatively shallow
175 deposition within the upper Campbell's Member while another is linked with the deeper water
176 (relative to the upper Campbell's Member) facies of the Cape Ann Member.

177 The large variations in $\delta^{34}\text{S}_{\text{sulfate}}$ evident in parts of the Port au Port strata warrant
178 consideration of secondary processes that could affect the S isotope composition of CAS.
179 $\delta^{18}\text{O}_{\text{carbonate}}$ is a useful indicator of geochemical alteration as ^{18}O -depleted signatures are often
180 attributed to post-depositional alteration resulting from isotopic exchange with meteoric fluids

181 (e.g., Given and Lohmann, 1985). The absence of any correlation between $\delta^{34}\text{S}_{\text{CAS}}$ and
182 $\delta^{18}\text{O}_{\text{carbonate}}$ suggests that post-depositional processes did not alter the S isotope composition of
183 CAS substantially. Furthermore, to a first order, $\delta^{34}\text{S}_{\text{pyrite}}$ is dictated by seawater sulfate $\delta^{34}\text{S}$.
184 Therefore, the large and sympathetic shifts in $\delta^{34}\text{S}_{\text{sulfate}}$ and $\delta^{34}\text{S}_{\text{pyrite}}$ (particularly in the lower part
185 of the section) supports the contention that $\delta^{34}\text{S}_{\text{sulfate}}$ is recording a primary seawater signal.

186

187 **6. Discussion**

188 *6.1 Ediacaran and Cambrian S isotopes and marine sulfate levels*

189 Several lines of evidence suggest that an Ediacaran increase in the oxidation state of the
190 ocean-atmosphere system led, perhaps for the first time in Earth history, to elevated seawater
191 sulfate concentrations. This evidence includes, but is not limited to, a shift in the abundance of
192 redox-sensitive elements (Canfield et al., 2007; Scott et al., 2008) and a substantial rise in the S
193 isotope difference between seawater sulfate and contemporaneously deposited sedimentary
194 pyrite ($\Delta^{34}\text{S}$) (Canfield and Teske, 1996; Hurtgen et al., 2005; Fike et al., 2006; Halverson and
195 Hurtgen, 2007; McFadden et al., 2008). Importantly, the extent of fractionation between
196 seawater sulfate and co-occurring sedimentary pyrite is controlled in large part by sulfate
197 availability. And, the amount of oxygen in the ocean atmosphere system is believed to exert a
198 primary control on marine sulfate levels because the primary source of seawater sulfate is
199 riverine input derived in part from the oxidative weathering of pyrite (e.g., Canfield, 2004). This
200 increase in $\Delta^{34}\text{S}$ (and by inference an increase in Earth surface oxygen levels) is evident in
201 Figure 3 and marked by a substantial decline in $\delta^{34}\text{S}_{\text{pyrite}}$ through the second half of the Ediacaran
202 Period, as recorded in sediments from Oman (Fike et al. 2006). $\Delta^{34}\text{S}$ decreases at the very end of
203 the Ediacaran period (Fike and Grotzinger, 2008) before increasing again in the earliest

204 Cambrian. [Note that this composite $\delta^{34}\text{S}$ (sulfate and pyrite) and $\delta^{13}\text{C}$ record does not include
205 all available data for the terminal Neoproterozoic due to poor age constraints for some samples.]

206 Sulfate levels may have dropped substantially during Early to Middle Cambrian time as
207 suggested by the chemical composition of fluid inclusions in halite (Horita et al., 2002;
208 Lowenstein et al., 2001, 2003; Brennan et al. 2004; Petrychenko et al., 2005) and ^{34}S -enriched
209 CAS (Kampschulte and Strauss, 2004; Gill et al., 2007), pyrite (Strauss, 1999) and francolite-
210 bound sulfate (Hough et al., 2006) in Early to Middle Cambrian sediments. The recognition of a
211 marked decrease in $\Delta^{34}\text{S}$ would corroborate the notion that marine sulfate levels fell at this time
212 (see discussion below). However, as Figure 3 illustrates, it is difficult to evaluate $\Delta^{34}\text{S}$ through
213 this interval due to a lack of previously published $\delta^{34}\text{S}_{\text{sulfate}}$ and $\delta^{34}\text{S}_{\text{pyrite}}$ generated in tandem
214 from the same stratigraphic section.

215

216 6.2 $\delta^{34}\text{S}_{\text{sulfate}}$, $\delta^{34}\text{S}_{\text{pyrite}}$, $\Delta^{34}\text{S}$ and Middle to Late Cambrian sulfate availability

217 The S isotope results from this study support the fluid inclusion (Horita et al., 2002;
218 Lowenstein et al., 2001, 2003; Brennan et al. 2004; Petrychenko et al., 2005) and previous S
219 isotope work (Strauss, 1999; Kampschulte and Strauss, 2004; Hough et al., 2006; Gill et al.,
220 2007) and suggest that sulfate concentrations in the Middle to Late Cambrian ocean were low
221 relative to terminal Neoproterozoic and modern values. The large and systematic shifts in
222 $\delta^{34}\text{S}_{\text{sulfate}}$ (>25‰) occur over relatively short geological timescales (<~2 m.y.; based on the
223 assumption that the entire section of Port au Port Group addressed in this study was deposited
224 over 5 to 10 million years) and are consistent with a seawater sulfate reservoir that was sensitive
225 to relatively short-term environmental perturbations (e.g., changes in pyrite burial and/or $\Delta^{34}\text{S}$).
226 Moreover, $\delta^{34}\text{S}_{\text{pyrite}}$ shifts in unison with $\delta^{34}\text{S}_{\text{sulfate}}$ through much of the section, but especially

227 through the March Point Formation and Cape Ann and Campbell's members of the Petit Jardin
228 Formation. To a first order, $\delta^{34}\text{S}_{\text{pyrite}}$ is dictated by seawater sulfate $\delta^{34}\text{S}$ and sympathetic
229 changes in $\delta^{34}\text{S}_{\text{sulfate}}$ and $\delta^{34}\text{S}_{\text{pyrite}}$ supports the contention that $\delta^{34}\text{S}_{\text{sulfate}}$ is changing over
230 relatively short stratigraphic distances (at least in this particular setting).

231 The S isotope difference between marine sulfate and contemporaneously deposited
232 sedimentary pyrite ($\Delta^{34}\text{S}$) provides further evidence for lower sulfate levels during this time
233 interval. The kinetic isotope effect associated with BSR, documented through experimental
234 studies (i.e., Detmers et al., 2001) and in natural systems (Habicht and Canfield, 1997; Habicht
235 and Canfield, 2001), leads to a fractionation of 2-46‰. In large part, the magnitude of this
236 fractionation is controlled by sulfate availability; larger fractionations are typically expressed
237 under non-limiting sulfate concentrations where microbes have a large reservoir of sulfate that
238 allows them to dissimilate ^{32}S preferentially. Smaller fractionations occur when sulfate is
239 limiting because sulfate-reducing microbes can alter the local sulfate reservoir (water column or
240 sediments) by extracting ^{32}S in the production of sulfide, thereby increasing the $\delta^{34}\text{S}$ composition
241 of residual sulfate and subsequently generated pyrite. Moreover, the capacity of sulfate-reducing
242 microbes to dissimilate ^{32}S in preference to ^{34}S decreases as sulfate concentrations fall below
243 ~50-200 μM (Habicht et al., 2002). Therefore, the overall effect of sulfate limitation is lower
244 $\Delta^{34}\text{S}$.

245 In order to achieve $\Delta^{34}\text{S} >46\%$, BSR must be accompanied by fractionations incurred
246 during the disproportionation of intermediate S species (e.g., S^0 , $\text{S}_2\text{O}_3^{2-}$; Jørgensen, 1990) that
247 results in sulfide depleted in ^{34}S relative to the initial reactant by an additional 7-20‰ (Canfield
248 and Thamdrup, 1994; Cypionka et al., 1998; Habicht et al., 1998; Böttcher et al., 2001).

249 Through repeated sulfide oxidation and disproportionation cycles, sulfide isotope values can
250 become depleted relative to sulfate by significantly more than 46‰.

251 While variable, Port au Port Group $\Delta^{34}\text{S}$ values average 23‰; all but three of the values
252 fall between 15 and 30‰ and none exceed 46‰. This average is both lower than the assumed
253 modern average value (35‰; Garrels and Lerman, 1984) and average values published for the
254 latest Neoproterozoic (~35‰; Fike et al., 2006). However, <46‰ values do not necessarily
255 indicate that S disproportionation was absent (i.e., Hurtgen et al., 2005, Johnston et al. 2005);
256 rather, they may relate to the efficiency with which sulfide is removed by reaction with Fe^{2+} ,
257 itself a function of seawater P_{O_2} (Hurtgen et al., 2005). It is important to note that the S isotope
258 composition of sedimentary pyrite is strongly influenced by local conditions and therefore these
259 modest $\Delta^{34}\text{S}$ values are not necessarily representative of a Middle to Late Cambrian average.
260 However, the low $\Delta^{34}\text{S}$ values in combination with the rapid shifts in $\delta^{34}\text{S}_{\text{sulfate}}$ and $\delta^{34}\text{S}_{\text{pyrite}}$ over
261 relatively short stratigraphic distances strongly support the notion that this particular basin
262 contained low sulfate concentrations.

263

264 *6.3 Relationship between $\delta^{13}\text{C}$, $\delta^{34}\text{S}$, and sulfate concentrations*

265 Very generally, $\delta^{13}\text{C}$ and $\delta^{34}\text{S}_{\text{sulfate}}$ are positively correlated through the Port au Port
266 strata, which suggests that the residence times of DIC and sulfate may have been roughly
267 comparable, at least in this basin. These positively correlated C and S isotope shifts may have
268 been driven by changes in OC burial and subsequent sympathetic changes in pyrite burial.
269 However, two deviations from the positive correlation exist and suggest, not surprisingly, that
270 the relationship between these two elemental cycles is more complex than outlined above.

271 The most obvious deviation occurs during the SPICE event, where the ~4‰ positive C
272 isotope excursion that straddles the Felix and Man O' War members is not accompanied by a
273 significant shift in $\delta^{34}\text{S}_{\text{sulfate}}$ (or $\delta^{34}\text{S}_{\text{pyrite}}$). While only five $\delta^{34}\text{S}_{\text{sulfate}}$ values were determined
274 through the SPICE event, it is important to note that one sample is coincident with the peak of
275 the $\delta^{13}\text{C}$ excursion. This pattern is very similar to that generated by the model we used to
276 ascertain changes in the coupled C and S system for the Cenozoic (Fig. 1); it would seem to
277 suggest that the residence time of sulfate in the ocean was much greater than that of DIC and
278 perhaps not drastically different from the modern ocean. However, the rapid $\delta^{34}\text{S}_{\text{sulfate}}$ shifts that
279 are present throughout this section (Fig. 2) are consistent with a sulfate reservoir more sensitive
280 to isotopic modification and it is unlikely that sulfate levels would increase through the SPICE
281 event given that the positive $\delta^{13}\text{C}$ excursion is thought to have been driven by an increase in OC
282 burial (Saltzman et al., 2004), providing more fuel for BSR. Moreover, in a separate section of
283 equivalent age deposited in an epicontinental sea elsewhere in Laurentia (Nevada), $\delta^{34}\text{S}_{\text{sulfate}}$ does
284 exhibit a positive excursion (>10‰) through the SPICE interval (Gill et al., 2007) and pre-
285 SPICE event $\delta^{13}\text{C}$ and $\delta^{34}\text{S}$ are elevated relative to Newfoundland strata. These contrasting
286 datasets from central and southern Laurentia suggest that the ocean was heterogeneous with
287 respect to $\delta^{34}\text{S}_{\text{sulfate}}$ (and $\delta^{13}\text{C}$) and so further supports the contention that Cambrian seawater
288 sulfate concentrations were low relative to modern values.

289 If marine sulfate concentrations were substantially lower in the Cambrian, why is it that
290 positive $\delta^{13}\text{C}$ excursions are recognized globally and $\delta^{34}\text{S}_{\text{sulfate}}$ excursions are not? One possible
291 explanation is that the residence time of seawater sulfate through this interval was significantly
292 lower than that of DIC, allowing for greater $\delta^{34}\text{S}_{\text{sulfate}}$ heterogeneity throughout the world oceans.
293 If we assume the residence time of DIC approximated modern values (~100 k.y.), and S fluxes

294 into and out of the ocean were similar to Cenozoic estimates ($\sim 1.5 \times 10^{18}$ moles/m.y.; Kurtz et
295 al., 2003), then sulfate levels must have been substantially $< \sim 100 \mu\text{M}$. If S fluxes into and out
296 of the ocean scaled proportionally with the marine sulfate reservoir and were lower during the
297 Cambrian, sulfate concentrations would have been even lower. Conversely, if the residence time
298 of DIC in the Cambrian ocean were higher than modern values (e.g., Berner, 2006), sulfate levels
299 could have been higher. For example, if the residence time of DIC in the Cambrian ocean was
300 500 k.y. (~ 5 x modern levels) and S fluxes into and out of the ocean were similar to Cenozoic
301 estimates, then sulfate levels must have been $< 525 \mu\text{M}$ in order for the residence time of sulfate
302 to be less than the residence time of DIC. Again, if S fluxes into and out of the ocean scaled
303 proportionally with sulfate levels and were lower, sulfate concentrations would have been
304 substantially $< 525 \mu\text{M}$. These sulfate concentrations are well below those estimated from fluid
305 inclusions encased in Cambrian halite (e.g., $\sim 5 - 12 \text{ mM}$; Horita et al., 2002; Lowenstein et al.,
306 2003, Brennan et al. 2004, Petrychenko et al., 2005). However, given the number of unknowns
307 (e.g., DIC residence time, S fluxes into and out of the ocean) we cannot rule out the possibility
308 that the residence time of seawater sulfate was less than the residence time of DIC during this
309 time.

310 Alternatively, the apparent heterogeneity in $\delta^{34}\text{S}_{\text{sulfate}}$ may indicate that one or both of
311 these environments (Newfoundland and/or Nevada) were somewhat restricted and not fully
312 tracking the S isotope composition of the global ocean. If so, however, why is it that sediments
313 from both localities record the $\delta^{13}\text{C}$ excursion across the SPICE event but the $\delta^{34}\text{S}_{\text{sulfate}}$ excursion
314 is expressed only in Nevada? One explanation may be linked to carbon exchange between
315 marine surface waters and the atmosphere. Over relatively short geologic timescales ($< 10^4$ y.r.),
316 the $\delta^{13}\text{C}$ composition of bulk atmospheric CO_2 is governed by carbon exchange with the

317 terrestrial biosphere and DIC in marine surface waters (e.g., Indermühle et al. 1999). Since
318 vascular land plants had not evolved in the Cambrian (e.g., Edwards 1979), the C isotope
319 composition of atmospheric CO₂ would have largely been dictated by equilibrium isotope
320 fractionations associated with air-sea gas exchange between the atmosphere and ocean (Mook,
321 1986). If $\delta^{13}\text{C}_{\text{DIC}}$ of marine surface waters were driven to substantially higher values for
322 hundreds of thousands of years—as they were during the SPICE event (Saltzman et al. 2004)—
323 the $\delta^{13}\text{C}$ composition of atmospheric CO₂ should have also increased by a corresponding, albeit
324 offset, amount. This ¹³C-enriched atmospheric CO₂ could then influence the surface waters of
325 basins not well connected to the open ocean and essentially transfer the $\delta^{13}\text{C}_{\text{carbonate}}$ excursion
326 generated in the open ocean to more restricted settings. The absolute $\delta^{13}\text{C}$ values of carbonates
327 surrounding the SPICE event in Newfoundland and Nevada are not the same but the magnitude
328 of the C isotope excursion is remarkably similar (~4‰). No similar mechanism is known for
329 expressing $\delta^{34}\text{S}_{\text{sulfate}}$ excursions generated in the open ocean to more restricted settings.
330 However, in order for the C isotope composition of DIC in an isolated basin to be buffered to the
331 atmosphere, the amount of C residing as DIC in the restricted basin must have been substantially
332 lower than the amount of CO₂ in the Cambrian atmosphere. Of course, neither the size of the
333 DIC reservoir nor Cambrian *p*CO₂ levels is known, and therefore, it is difficult to evaluate the
334 reasonableness of this explanation.

335 The second instance where C and S isotopes appear to deviate from positively correlated
336 changes is in the March Point Formation where a 15 ‰ decrease in $\delta^{34}\text{S}_{\text{sulfate}}$ (and $\delta^{34}\text{S}_{\text{pyrite}}$)
337 precedes a ~4‰ fall in $\delta^{13}\text{C}$ (Fig. 2). This is an intriguing result and again may indicate that
338 sulfate levels were sufficiently low in this basin and that the characteristic response time for
339 $\delta^{34}\text{S}_{\text{sulfate}} < \delta^{13}\text{C}_{\text{DIC}}$. In other words, a decrease in OC burial may have influenced $\delta^{34}\text{S}_{\text{sulfate}}$ more

340 rapidly than $\delta^{13}\text{C}$ by reducing pyrite burial rates. While time constraints are poor through this
341 interval, the lag time between the initial $\delta^{34}\text{S}$ drop and $\delta^{13}\text{C}$ fall is represented by ~25 m of
342 section and likely represents too much time ($>10^4$ y.r.) for this to be reasonable if the residence
343 time of DIC was between 100 and 500 k.y. Alternatively, the $\delta^{34}\text{S}_{\text{sulfate}}$ decline may not have
344 been directly and/or immediately linked to perturbations of the C cycle. For example, $\delta^{34}\text{S}_{\text{sulfate}}$
345 variations are typically attributed to changes in pyrite burial rates facilitated by changes in OC
346 availability. However, in the modern ocean, pyrite burial efficiency is quite low; as much as
347 95% of sulfide generated during BSR is reoxidized to sulfate and intermediate S species
348 (Jørgensen et al., 1990). Within this context, pyrite burial rates may oscillate substantially if the
349 percentage of BSR-generated sulfide that is oxidized to sulfate and intermediate S species
350 varies—even if global rates of BSR remain constant.

351 Turchyn and Schrag (2004) argued that fluctuations in the oxygen isotope composition of
352 seawater sulfate over the last 10 m.y. can be attributed to changes in the extent and means by
353 which sulfide has been reoxidized on continental margins. These high frequency changes in
354 pyrite burial efficiency have had little to no effect on $\delta^{34}\text{S}_{\text{sulfate}}$ over the last 10 m.y. due to the
355 large residence time of sulfate over this time interval (e.g., Paytan et al., 1998). However, if the
356 Cambrian ocean had much lower sulfate concentrations, changes in the balance between sulfide
357 production (via BSR) and reoxidation could have affected $\delta^{34}\text{S}_{\text{sulfate}}$ considerably on shorter (<1
358 m.y.) geological timescales. An important control on the extent of sulfide reoxidation is oxygen
359 availability in the marine system and it has been argued that globally extensive black shale
360 deposition in the Middle and Upper Cambrian resulted from poor ventilation of the deep oceans
361 during a greenhouse climate (Berry and Wilde, 1978). The $\delta^{34}\text{S}$ drop that proceeds the $\delta^{13}\text{C}$ fall
362 in the March Point Formation may have been induced by changes in pyrite burial efficiency

363 facilitated by subtle changes in Cambrian marine redox that influenced the S cycle before (and/or
364 to a greater extent than) the C cycle. This discussion is expanded below. More specifically, we
365 explore how oceanic redox might influence the C/S burial ratio and $\Delta^{34}\text{S}$ on a global scale in a
366 way that would facilitate larger $\delta^{34}\text{S}_{\text{sulfate}}$ excursions per mole of OC burial.

367

368 *6.4 Modeling insights*

369 Here, we utilize the simple reservoir- and time-dependent mass balance equations for
370 $\delta^{13}\text{C}$ and $\delta^{34}\text{S}_{\text{sulfate}}$ (equations 1 and 2) to understand better the relationship between sulfate
371 residence time and $\delta^{34}\text{S}_{\text{sulfate}}$ response to perturbations to the Cambrian C cycle. More
372 specifically, how low must sulfate concentrations have been (assuming Cenozoic inputs and
373 outputs of S to and from the marine system) to generate the $>10\%$ $\delta^{34}\text{S}_{\text{sulfate}}$ shifts expressed in
374 the Cambrian data presented in Figure 2 and yet remain consistent with the modest, but not
375 negligible, $\Delta^{34}\text{S}$ values? In the following simulations, we assume the $>10\%$ $\delta^{34}\text{S}_{\text{sulfate}}$ variations
376 were global in extent; however, as already discussed, it is possible that the Newfoundland $\delta^{34}\text{S}$
377 signal records local perturbations not necessarily linked to the global ocean. Nonetheless, this
378 exercise highlights important aspects of the relationships among $\delta^{13}\text{C}$, $\delta^{34}\text{S}$, and $\Delta^{34}\text{S}$ in a low
379 sulfate ocean.

380 The sensitivity of $\delta^{34}\text{S}_{\text{sulfate}}$ to a stepwise, 50% increase in F_{org} and F_{py} for 1 m.y. (during
381 the interval 2 to 3 m.y., represented by gray band) is explored under varying initial sulfate
382 concentrations (Fig. 4). As earlier, initial conditions were constructed using mass, flux and
383 isotope compositions believed to represent Cenozoic C and S cycles (Kurtz et al., 2003).
384 However, here we prescribe lower initial sulfate levels (0.28 mM, 1.9 mM and 3.5 mM) and a
385 lower $\Delta^{34}\text{S}$ (25‰ rather than 35‰) that approximates the average recorded in Port Au Port

386 Group sediments and is more consistent with a low sulfate ocean. The reduced $\Delta^{34}\text{S}$ forces a
387 lower steady state $\delta^{34}\text{S}_{\text{sulfate}}$ value (17.7‰) but more importantly it reduces the magnitude of
388 $\delta^{34}\text{S}_{\text{sulfate}}$ excursions generated per mole of OC buried. The C and S cycles are again linked using
389 a constant C/S burial ratio of 7.7. [Raiswell and Berner (1986) challenged constant C/S and we
390 explore the consequences of relaxing this assumption below.] Although not shown in Figure 4,
391 the 50% increase in F_{org} forces a 2.8‰ positive excursion in $\delta^{13}\text{C}$ as shown in Figure 1.

392 The model results indicate that even at very low initial sulfate concentrations (280 μM , τ
393 = 0.27 m.y.), a 50% increase in OC and pyrite burial prompts only an $\sim 5\%$ $\delta^{34}\text{S}_{\text{sulfate}}$ excursion.
394 In three of the four runs, $\Delta^{34}\text{S}$ was held constant at 25‰. However, in run 1a (Fig. 4), we
395 include a stepwise decrease in $\Delta^{34}\text{S}$ from 25 to 15‰ once sulfate concentrations drop to < 200
396 μM (e.g., Habicht et al., 2002). This forces $\delta^{34}\text{S}_{\text{sulfate}}$ to decrease abruptly within the OC burial
397 event and ultimately bring about an $\sim 8\%$ decline over 1 m.y. This underscores an interesting
398 aspect of S cycling in low sulfate oceans: the sensitivity of $\Delta^{34}\text{S}$ to fluctuating ocean chemistries
399 and its influence on the S isotope evolution of seawater sulfate.

400 Previous work suggests that the Middle to Upper Cambrian ocean may have been more
401 susceptible to at least regional anoxia. Berry and Wilde (1978) argued that extensive black shale
402 deposition in the Cambrian resulted from poor ventilation of the deep oceans due to minimal sea
403 ice formation at high latitudes. Similarly, Saltzman (2005) suggested that extended ($>10^7$ y.r.)
404 periods of relative $\delta^{13}\text{C}$ stability found in much of the Middle and Upper Cambrian resulted from
405 nitrogen limitation in a greenhouse climate that promoted reduced O_2 solubility in marine waters
406 and increased denitrification as result of water column anoxia. Furthermore, Raiswell and
407 Berner (1986) found that C/S ratios in Cambrian aged marine shales were lower (~ 0.5) than

408 those recorded during any other period during the Phanerozoic (modern = 2.8). They attributed
409 reduced C/S to euxinic conditions.

410 If the chemocline were raised into the water column during times of enhanced OC
411 production in the Cambrian, syngenetic (water column) pyrite formation may have occurred.
412 This has important implications for evaluating the relationship between the Cambrian C and S
413 isotope record for two reasons. First, sediments deposited under euxinic conditions are
414 characterized by reduced C/S as result of syngenetic pyrite formation that is decoupled from the
415 amount of OC buried in the sediments (Leventhal, 1983; Raiswell and Berner, 1985). Under
416 these circumstances, Fe is often the limiting factor in pyrite formation rather than OC (Raiswell
417 and Berner, 1985). Second, if a significant fraction of pyrite ultimately buried in the sediments
418 formed syngenetically, $\Delta^{34}\text{S}$ values may have shifted to significantly higher values. This is
419 because sulfate-reducing bacteria have a much larger reservoir of sulfate from which to
420 dissimilate the lighter ^{32}S versus ^{34}S (e.g., Lyons, 1997; the effect is seen in mid-Proterozoic S
421 isotope data of Shen et al., 2003). Within this context, if the Cambrian ocean was susceptible to
422 periods of euxinia, C/S ratios likely decreased and $\Delta^{34}\text{S}$ may have increased (assuming sulfate
423 levels were not brought too low during the event), permitting much larger S isotope shifts in
424 seawater sulfate per mole of C buried.

425 As earlier, the sensitivity of $\delta^{34}\text{S}_{\text{sulfate}}$ to a stepwise, 50% increase in F_{org} for 1 m.y. is
426 explored under varying initial sulfate concentrations (Fig. 5). However, in order to account for
427 an increase in syngenetic pyrite formation resulting from anoxia, F_{py} increases 100% through the
428 OC burial event and $\Delta^{34}\text{S}$ increases from 25 to 30‰. As a result, larger $\delta^{34}\text{S}_{\text{sulfate}}$ excursions are
429 expressed per mole of OC buried. A ~13‰ $\delta^{34}\text{S}_{\text{sulfate}}$ increase is generated over 1 m.y. when
430 initial sulfate levels are set at 700 μM ($\tau = 0.67$ m.y.).

431 Given these preliminary modeling results, it appears that $> 10\text{‰}$ global $\delta^{34}\text{S}_{\text{sulfate}}$ shifts
432 may be generated by OC burial events (F_{org} increases by 50%) at sulfate levels approaching 1
433 mM if C/S and $\Delta^{34}\text{S}$ are allowed to fluctuate as a result of water column anoxia. Of course, this
434 is a crude estimate that assumes we have some control on the residence time of DIC in the
435 Cambrian as well as S fluxes into and out of the ocean—which we do not. In fact, if S fluxes
436 into and out of the ocean were scaled proportionally with the marine sulfate reservoir and were
437 lower in the Cambrian, the residence time of sulfate would have been higher (similar to Cenozoic
438 values), making it more difficult to generate $> 10\text{‰}$ $\delta^{34}\text{S}_{\text{sulfate}}$ excursions (e.g., Fig. 1). We are
439 not necessarily advocating a particular sulfate concentration for Late Cambrian seawater.
440 Rather, we are suggesting that sulfate levels were low relative to modern values, that decreased
441 residence time for S and, possibly, increased residence time for C are necessary to understand the
442 relationships between C and S isotopes, and perhaps most importantly, basinal anoxia must be
443 invoked in the models to reproduce the geochemical signatures preserved in the Port au Port
444 strata. Furthermore, the interpretations developed in this study are only based on two sections in
445 relatively shallow seas bordering Laurentia (Newfoundland and Nevada; Gill et al., 2007).
446 Future work should focus on reconstructing the temporal and spatial evolution of $\delta^{13}\text{C}$ and $\delta^{34}\text{S}$
447 (sulfate and pyrite) through multiple sections of early Paleozoic strata in order to constrain the
448 mechanistic details underpinning the geochemical evolution of the C and S cycles. Nonetheless,
449 these two data sets, coupled with simple modeling results, do highlight some interesting
450 dynamics relating OC burial, sulfate concentrations, ocean redox, $\Delta^{34}\text{S}$ and ultimately $\delta^{34}\text{S}_{\text{sulfate}}$.

451

452 6.5 *Relationships among sulfate levels, atmospheric O_2 and Cambrian life*

453 The Early Paleozoic represents one of the most dynamic times in the history of complex
454 life. Within the first 25 million years of the Cambrian Period, animals with mineralized
455 skeletons diversified and the first metazoan reefs were established. This major diversification,
456 known as the Cambrian Explosion, was disrupted by major extinctions near the end of the Early
457 Cambrian (e.g., Zhuravlev and Wood, 1996). These extinctions decimated the archaeocyathids
458 and other massively calcified reef builders and also marked the last appearances of many so-
459 called small shelly fossils (but see Porter, 2004, for discussion of taphonomic bias). For the
460 ensuing ~40 million years of the Middle to Late Cambrian and earliest Ordovician, the
461 abundance of skeletons was low in marine carbonates (Li and Droser, 1997, 1999), animal reefs
462 were absent (Rowland and Shapiro, 2002) and turnover rates were unusually high (Bambach et
463 al., 2004). What makes this interval enigmatic is that it postdates the origins of both the major
464 animal body plans and the evolution of calcified skeletons within many of them, but predates the
465 major Ordovician radiation that established skeletons as major sinks for calcium carbonate.

466 If an increase in the oxidation state of the coupled ocean-atmosphere system paved the
467 way for the evolution and radiation of macroscopic Metazoa in the Ediacaran (e.g., Knoll and
468 Carroll, 1999; Canfield et al., 2007; Fike et al., 2006), it is reasonable to ask if changes in marine
469 redox profiles during the Early to Middle Cambrian and into the Ordovician governed the demise
470 and delayed recovery of skeletonized animals (e.g., Zhuravlev and Wood, 1996; Pruss et
471 al., 2007). Several lines of evidence suggest that marine waters were more susceptible to
472 episodes of anoxia during this time, including extensive black shale deposition (Berry and Wilde,
473 1978), increased seawater temperatures and therefore lower O₂ solubility (Berry and Wilde,
474 1978; Saltzman 2005; Trotter et al., 2008), and reduced C/S in Cambro-Ordovician marine shales
475 (Raiswell and Berner, 1986). Furthermore, the C and S isotope models presented in this study

476 indicate that fluctuating water column anoxia in a low sulfate ocean generates the largest $\delta^{34}\text{S}$
477 excursions per mole of OC produced/buried consistent with the $\delta^{13}\text{C}$ and $\delta^{34}\text{S}_{\text{sulfate}}$ shifts
478 expressed in the Port au Port carbonates of Newfoundland. Collectively, these results suggest
479 that reduced oxygen levels in subsurface water masses may have played a significant role in late
480 Early Cambrian extinction and the delayed recovery of animal reefs and skeletonized animals,
481 arguably by decreasing the saturation state of surface waters with respect to carbonate minerals
482 (Fischer et al. 2007, Higgins and Schrag, 2007; see Pruss et al., 2007, for explicit discussion of
483 Cambro-Ordovician oceans). Continuing geochemical research will help to determine the
484 environmental context of major events in both Cambrian and Ordovician skeletal evolution.

485

486 **7. Conclusions**

487 A significant increase in $\Delta^{34}\text{S}$, as recorded in terminal Neoproterozoic rocks, suggests
488 that an increase in the oxidation state of the ocean-atmosphere system facilitated an increase in
489 seawater sulfate concentrations just prior to the appearance of the Ediacaran Fauna (Fike et al.,
490 2006). Sulfate levels, however, may have dropped substantially during the Early to Middle
491 Cambrian (Horita et al., 2002; Lowenstein et al., 2001, 2003; Brennan et al., 2004; Kampschulte
492 and Strauss, 2004; Petrychenko et al., 2005; Hough et al., 2006; Gill et al., 2007). S isotope
493 results presented in this study support these findings; reduced $\Delta^{34}\text{S}$, large $\delta^{34}\text{S}_{\text{sulfate}}$ shifts over
494 relatively short stratigraphic intervals, and a general positive coupling between $\delta^{13}\text{C}_{\text{carbonate}}$ and
495 $\delta^{34}\text{S}_{\text{sulfate}}$ all suggest that the Middle to Late Cambrian sulfate reservoir was more sensitive to
496 change than either terminal Neoproterozoic or Cenozoic oceans.

497 A simple C and S isotope box model illustrates that low sulfate concentrations alone fail
498 to account for the $>10\text{‰}$ $\delta^{34}\text{S}_{\text{sulfate}}$ shifts recognized in the Port au Port Group strata. These

499 larger $\delta^{34}\text{S}$ shifts can be generated if fluctuating oceanic redox is invoked, whereby marine
500 anoxia forces reduced C/S and elevated $\Delta^{34}\text{S}$, resulting in larger $\delta^{34}\text{S}$ changes per mole of OC
501 buried. The emerging environmental picture of the later Cambrian Earth system suggests that
502 the delayed recovery of organisms with carbonate skeletons and animal reefs following late
503 Early Cambrian extinction may have been due in part to fluctuating marine redox and reduced
504 oxygen levels in the coupled ocean-atmosphere system.

505 Ultimately, the relationship between the geochemical cycles of C and S represent a
506 complex set of feedbacks that operate on a variety of timescales. The Middle to Late Cambrian
507 ocean presents an opportunity to investigate the driving forces behind C and S isotopic change in
508 oceans unlike those we know today (i.e., through most of Earth history).

509

510 **Acknowledgements**

511 We thank the Agouron Institute (postdoctoral fellowship to SP) and NSF Grant DES
512 0420592 (AHK) for partial funding of this research. We also thank Greg Eiseid and Dan
513 Schrag for assistance with carbon and oxygen isotope analyses and David Fike, an anonymous
514 reviewer and P. Delaney for comments that improved the content and clarity of this manuscript.

515

516 **References Cited**

- 517 Ault, W.U. and Kulp, J.L., 1959. Isotopic geochemistry of sulphur. *Geochimica et*
518 *Cosmochimica Acta* 16, 201-235.
- 519 Bambach, R.K., Knoll, A.H. and Wang, S.M., 2004. Origination, extinction, and mass depletions
520 of marine diversity. *Paleobiology* 30, 522-542.
- 521 Berner, E.K. and Berner, R.A., 1996. *Global Environment*. Prentice Hall, Upper Saddle River,
522 NJ, 376 pp.
- 523 Berner, R.A., 1987. Models for carbon and sulfur cycles and atmospheric oxygen: application to
524 Paleozoic geologic history. *American Journal of Science* 287, 177-196.
- 525 Berner, R.A., 2006. GEOCARBSULF: A combined model for Phanerozoic atmospheric O₂ and
526 CO₂. *Geochimica et Cosmochimica Acta* 70, 5653-5664.
- 527 Berner, R.A. and Raiswell, R., 1983. Burial of organic carbon and pyrite sulfur in sediments over
528 Phanerozoic time: a new theory. *Geochimica et Cosmochimica Acta* 47, 855-862.
- 529 Berry, W.B.N. and Wilde, P., 1978. Progressive ventilation of the oceans-An explanation for the
530 distribution of the lower Paleozoic black shales. *American Journal of Science* 278, 257-
531 275.
- 532 Böttcher, M.E., Thamdrup, B. and Vennemann, T.W., 2001. Oxygen and sulfur isotope
533 fractionation during anaerobic bacterial disproportionation of elemental sulfur.
534 *Geochimica et Cosmochimica Acta* 65, 1601-1609.
- 535 Brennan, S.T., Lowenstein, T.K. and Horita, J., 2004. Seawater chemistry and the advent of
536 biocalcification. *Geology* 32, 473-476.

537 Burdett, J.W., Arthur, M.A. and Richardson, M., 1989. A Neogene seawater sulfur isotope age
538 curve from calcareous pelagic microfossils. *Earth and Planetary Science Letters* 94, 189-
539 198.

540 Canfield, D.E., 2004. The evolution of the Earth surface sulfur reservoir. *American Journal of*
541 *Science* 304, 839-861.

542 Canfield, D.E., Poulton, S.W. and Narbonne, G.M., 2007. Late Neoproterozoic deep-ocean
543 oxygenation and the rise of animal life. *Science* 315, 92-95.

544 Canfield, D.E., Raiswell, R., Westrich, J.T., Reaves, C.M. and Berner, R.A., 1986. The use of
545 chromium reduction in the analysis of reduced inorganic sulfur in sediments and shales.
546 *Chemical Geology* 54, 149-155.

547 Canfield, D.E. and Teske, A., 1996. Late Proterozoic rise in atmospheric oxygen concentration
548 inferred from phylogenetic and sulphur-isotope studies. *Nature* 382, 127-132.

549 Canfield, D.E. and Thamdrup, B., 1994. The production of ³⁴S-depleted sulfide during bacterial
550 disproportionation of elemental sulfur. *Science* 266, 1973-1975.

551 Chow, N. and James, N.P., 1987. Facies-specific, calcitic and bimineralic ooids from Middle and
552 Upper Cambrian platform carbonates, western Newfoundland, Canada. *Journal of*
553 *Sedimentary Petrology* 57, 907-921.

554 Cowan, C.A. and James, N.P., 1993. The interactions of sea-level change, terrigenous-sediment
555 influx, and carbonate productivity as controls on Upper Cambrian Grand Cycles of
556 western Newfoundland, Canada. *Geological Society of America Bulletin* 105, 1576-
557 1590.

558 Cypionka, H., Smock, A.M. and Böttcher, M.E., 1998. A combined pathway of sulfur compound
559 disproportionation in *Desulfovibrio desulfuricans*. *FEMS Microbiology Ecology* 166,
560 181-186.

561 Derry, L.A., Brasier, M., Corfield, R., Rozanov, A. and Zhuravlev, A., 1994. Sr and C isotopes
562 in Lower Cambrian carbonates from the Siberian craton: a paleoenvironmental record
563 during the "Cambrian explosion". *Earth and Planetary Science Letters* 128, 671-681.

564 Detmers, J., Brüchert, V., Habicht, K.S. and Kuever, J., 2001. Diversity of sulfur isotope
565 fractionations by sulfate-reducing prokaryotes. *Applied and Environmental Microbiology*
566 67, 888-894.

567 Edwards, D., 1979. The early history of vascular plants based on Late Silurian and Early
568 Devonian floras of the British Isles. In: A.L. Harris, C.H. Holland and B.E. Leake
569 (Editors), *The Caledonides of the British Isles-reviewed*. Geological Society of London
570 Special Publication, pp. 405-410.

571 Fike, D.A. and Grotzinger, J.P., 2008. A paired sulfate—pyrite $\delta^{34}\text{S}$ approach to understanding
572 the evolution of the Ediacaran—Cambrian sulfur cycle. *Geochimica et Cosmochimica*
573 *Acta* 72, 2636-2648.

574 Fike, D.A., Grotzinger, J.P., Pratt, L.M. and Summons, R.E., 2006. Oxidation of the Ediacaran
575 Ocean. *Nature* 444, 744-747.

576 Fischer, W., Higgins, J. and Pruss, S., 2007. Delayed biotic recovery from the Permian-Triassic
577 extinction may have been influenced by a redox-driven reorganization of the marine
578 carbonate system, Geological Society of America, Abstracts with Programs, pp. 420.

579 Garrels, R.M. and Lerman, A., 1984. Coupling of sedimentary sulfur and carbon cycles-an
580 improved model. *American Journal of Science* 284, 989-1007.

581 Gill, B.C., Lyons, T.W. and Saltzman, M.R., 2007. Parallel, high-resolution carbon and sulfur
582 isotope records of the evolving Paleozoic marine sulfur reservoir. *Palaeogeography,*
583 *Palaeoclimatology, Palaeoecology* 256, 156-173.

584 Given, R.K. and Lohmann, K.C., 1985. Derivation of the original isotopic composition of
585 Permian marine cements. *Journal of Sedimentary Petrology* 55, 430-439.

586 Gorjan, P., Veevers, J.J. and Walter, M.R., 2000. Neoproterozoic sulfur-isotope variation in
587 Australia and global implications. *Precambrian Research* 100, 151-179.

588 Habicht, K.S. and Canfield, D.E., 1997. Sulfur isotope fractionation during bacterial sulfate
589 reduction in organic-rich sediments. *Geochimica et Cosmochimica Acta* 61, 5351-5361.

590 Habicht, K.S. and Canfield, D.E., 2001. Isotope fractionation by sulfate-reducing natural
591 populations and the isotopic composition of sulfide in marine sediments. *Geology* 29,
592 555-558.

593 Habicht, K.S., Canfield, D.E. and Rethmeier, J., 1998. Sulfur isotope fractionation during
594 bacterial reduction and disproportionation of thiosulfate and sulfite. *Geochimica et*
595 *Cosmochimica Acta* 62, 2585-2595.

596 Habicht, K.S., Gade, M., Thamdrup, B., Berg, P. and Canfield, D.E., 2002. Calibration of sulfate
597 levels in the Archean ocean. *Science* 298, 2372-2374.

598 Halverson, G.P., Hoffman, P.F., Schrag, D.P., Maloof, A.C. and Rice, A.H., 2005. Towards a
599 Neoproterozoic composite carbon isotope record. *Geological Society of America Bulletin*
600 117, 1181-1207.

601 Halverson, G.P. and Hurtgen, M.T., 2007. Ediacaran growth of the marine sulfate reservoir.
602 *Earth and Planetary Science Letters* 263, 32-44.

603 Hayes, J.M., Strauss, H. and Kaufman, A.J., 1999. The abundance of ^{13}C in marine organic
604 matter and isotopic fractionation in the global biogeochemical cycle of carbon during the
605 past 800 Ma. *Chemical Geology* 161, 103-125.

606 Higgins, J. and Schrag, D., 2007. CaCO_3 cycling in anoxic oceans, Geological Society of
607 America, Abstracts with Programs, pp. 420.

608 Holland, H.D., 1973. Systematics of the isotopic composition of sulfur in the oceans during the
609 Phanerozoic and its implications for atmospheric oxygen. *Geochimica et Cosmochimica*
610 *Acta* 37, 2605-2616.

611 Holland, H.D., 1984. *The Chemical Evolution of the Atmosphere and Oceans*. Princeton
612 University Press, Princeton, NJ, 582 pp.

613 Holser, W.T., Maynard, J.B. and Cruikshank, K.M., 1989. Modelling the Natural Cycle of
614 Sulphur Through Phanerozoic Time. In: P. Brimblecombe and A.Y. Lein (Editors),
615 *Evolution of the Global Biogeochemical Sulphur Cycle*. John Wiley & Sons Ltd, pp. 21-
616 56.

617 Horita, J., Zimmermann, H. and Holland, H.D., 2002. Chemical evolution of seawater during the
618 Phanerozoic: Implications from the record of marine evaporites. *Geochimica et*
619 *Cosmochimica Acta* 66, 3733-3756.

620 Hough, M.L. et al., 2006. A major sulphur isotope event at c. 510 Ma: a possible anoxia-
621 extinction-volcanism connection during the Early-Middle Cambrian transition? *Terra*
622 *Nova* 18, 257-263.

623 Hurtgen, M.T., Arthur, M.A. and Halverson, G.P., 2005. Neoproterozoic sulfur isotopes, the
624 evolution of microbial sulfur species, and the burial efficiency of sulfide as sedimentary
625 pyrite. *Geology* 33, 41-44.

626 Hurtgen, M.T., Arthur, M.A., Suits, N.S. and Kaufman, A.J., 2002. The sulfur isotopic
627 composition of Neoproterozoic seawater sulfate: Implications for a snowball Earth? *Earth*
628 and *Planetary Science Letters* 203, 413-430.

629 Hurtgen, M.T., Halverson, G.P., Arthur, M.A. and Hoffman, P.F., 2006. Sulfur cycling in the
630 aftermath of a 635-Ma snowball glaciation: Evidence for a syn-glacial sulfidic deep
631 ocean. *Earth and Planetary Sciences* 245, 551-570.

632 Indermühle, A. et al., 1999. Holocene carbon-cycle dynamics based on CO₂ trapped in ice at
633 Taylor Dome, Antarctica. *Nature* 398, 121-126.

634 Johnston, D.T. et al., 2005. Active microbial sulfur disproportionation in the Mesoproterozoic.
635 *Science* 310, 1477-1479.

636 Jørgensen, B.B., 1990. A thiosulfate shunt in the sulfur cycle of marine sediments. *Science* 249,
637 152-154.

638 Kah, L.C., Lyons, T.W. and Frank, T.D., 2004. Low marine sulphate and protracted oxygenation
639 of the Proterozoic biosphere. *Nature* 431, 834-838.

640 Kampschulte, A. and Strauss, H., 2004. The sulfur isotopic evolution of Phanerozoic seawater
641 based on the analysis of structurally substituted sulfate in carbonates. *Chemical Geology*
642 204, 255-286.

643 Knoll, A. and Carroll, S., 1999. Early animal evolution: emerging views from comparative
644 biology and geology. *Science* 284, 2129-2137.

645 Knoll, A.H., 2003. Biomineralization and evolutionary history. In: P.A. Dove, J.D. Yoreo and S.
646 Weiner (Editors), *Biomineralization*. Mineralogical Society of America, Washington,
647 DC, pp. 329-356.

648 Kump, L.R. and Arthur, M.A., 1999. Interpreting carbon-isotope excursions: carbonates and
649 organic matter. *Chemical Geology* 161, 181-198.

650 Kump, L.R. and Garrels, R.M., 1986. Modeling atmospheric O₂ in the global sedimentary redox
651 cycle. *American Journal of Science* 286, 337-360.

652 Kurtz, A.C., Kump, L.R., Arthur, M.A., Zachos, J.C. and Paytan, A., 2003. Early Cenozoic
653 decoupling of the global carbon and sulfur cycles. *Paleoceanography* 18.

654 Leventhal, J.S., 1983. An interpretation of carbon and sulfur relationships in Black Sea
655 sediments as indicators of environments of deposition. *Geochimica et Cosmochimica*
656 *Acta* 47, 133-137.

657 Li, X. and Droser, M.L., 1997. Nature and distribution of Cambrian shell concentrations:
658 Evidence from the Basin and Range Province of the Western United States (California,
659 Nevada, and Utah). *Palaios* 12, 111-126.

660 Li, X. and Droser, M.L., 1999. Lower and Middle Ordovician shell beds from the Basin and
661 Range province of the western United States (California, Nevada, and Utah). *Palaios* 14,
662 215-233.

663 Lowenstein, T.K., Hardie, L.A., Timofeeff, M.N. and Demicco, R.V., 2003. Secular variation in
664 seawater chemistry and the origin of calcium chloride basinal brines. *Geology* 31, 857-
665 860.

666 Lowenstein, T.K., Timofeeff, M.N., Brennan, S.T., Hardie, L.A. and Demicco, R.V., 2001.
667 Oscillations in Phanerozoic seawater chemistry: Evidence from fluid inclusions. *Science*
668 294, 1086-1088.

669 Lyons, T.W., 1997. Sulfur isotopic trends and pathways of iron sulfide formation in upper
670 Holocene sediments of the anoxic Black Sea. *Geochimica et Cosmochimica Acta* 61,
671 3367-3382.

672 McFadden, K.A. et al., 2008. Pulsed oxidation and biological evolution in the Ediacaran
673 Doushantuo Formation. *Proceedings of the National Academy of Science* 105, 3197-
674 3202.

675 Mook, W.G., 1986. ^{13}C in atmospheric CO_2 . *Netherlands Journal of Sea Research* 20, 211-223.

676 Paytan, A., Kastner, M., Campbell, D. and Thiemens, M.H., 1998. Sulfur isotopic composition of
677 Cenozoic seawater sulfate. *Science* 282, 1459-1462.

678 Paytan, A., Kastner, M., Campbell, D. and Thiemens, M.H., 2004. Seawater sulfur isotope
679 fluctuations in the Cretaceous. *Science* 304, 1663-1665.

680 Petrychenko, O.Y., Peryt, T.M. and Chechel, E.I., 2005. Early Cambrian seawater chemistry
681 from fluid inclusions in halite from Siberian evaporites. *Chemical Geology* 219, 149-161.

682 Porter, S.M., 2004. Closing the phosphatization window: testing for the influence of taphonomic
683 megabias on the pattern of small shelly fossil decline. *Palaios* 19, 178-183.

684 Pruss, S., Finnegan, S., Fischer, W. and Knoll, A., submitted. Carbonates in skeleton-poor seas:
685 New insights from Cambrian and Ordovician strata of Laurentia. *Palaios*.

686 Raab, M. and Spiro, B., 1991. Sulfur isotopic variations during seawater evaporation with
687 fractional crystallization. *Chemical Geology* 86, 323-333.

688 Raiswell, R. and Berner, R.A., 1985. Pyrite formation in euxinic and semi-euxinic sediments.
689 *American Journal of Science* 285, 710-724.

690 Raiswell, R. and Berner, R.A., 1986. Pyrite and organic matter in Phanerozoic normal marine
691 shales. *Geochimica et Cosmochimica Acta* 50, 1967-1976.

692 Rees, C.E., Jenkins, W.J. and Monster, J., 1978. The sulphur isotopic composition of ocean
693 water sulphate. *Geochimica et Cosmochimica Acta* 42, 377-381.

694 Rowland, S.M. and Shapiro, R.S., 2002. Reef patterns and environmental influences in the
695 Cambrian and earliest Ordovician. In: W. Kiessling, E. Flügel and J. Golonka (Editors),
696 *Phanerozoic Reef Patterns*, Tulsa, pp. 95-128.

697 Saltzman, M.R., 2005. Phosphorus, nitrogen, and the redox evolution of Paleozoic oceans.
698 *Geology* 33, 573-576.

699 Saltzman, M.R. et al., 2004. The Late Cambrian SPICE event and the Sauk II-Sauk III
700 regression: New evidence from Laurentian basins in Utah, Iowa and Newfoundland.
701 *Journal of Sedimentary Research* 74, 366-377.

702 Saltzman, M.R. et al., 2000. A global carbon isotope excursion (SPICE) during the Late
703 Cambrian: relation to trilobite extinctions, organic-matter burial and sea level.
704 *Palaeogeography Palaeoclimatology Palaeoecology* 162, 211-223.

705 Schröder, S., Schreiber, B.C., Amthor, J.E. and Matter, A., 2004. Stratigraphy and environmental
706 conditions of the terminal Neoproterozoic-Cambrian Period in Oman: evidence from
707 sulphur isotopes. *Journal of the Geological Society, London* 161, 489-499.

708 Scott, C. et al., 2008. Tracing the stepwise oxygenation of the Proterozoic ocean. *Nature* 452,
709 456-459.

710 Shen, Y., Knoll, A.H. and Walter, M.R., 2003. Evidence for low sulphate and anoxia in a mid-
711 Proterozoic marine basin. *Nature* 423, 632-635.

712 Strauss, H., 1999. Geological evolution from isotope proxy signals-sulfur. *Chemical Geology*
713 161, 89-101.

- 714 Trotter, J.A., Williams, I.S., Barnes, C.R., Lécuyer, C. and Nicoll, R.S., 2008. Did cooling
715 oceans trigger Ordovician biodiversification? Evidence from conodont thermometry.
716 Science 321, 550-554.
- 717 Turchyn, A.V. and Schrag, D.P., 2004. Oxygen isotope constraints on the sulfur cycle over the
718 past 10 million years. Science 303, 2004-2007.
- 719 Veizer, J., Holser, W.T. and Wilgus, C.K., 1980. Correlation of $^{13}\text{C}/^{12}\text{C}$ and $^{34}\text{S}/^{32}\text{S}$ secular
720 variations. Geochimica et Cosmochimica Acta 44, 579-587.
- 721 Zhuravlev, A. and Wood, R., 1996. Anoxia as the cause of the mid-early Cambrian (Botomian)
722 extinction event. Geology 24, 311-314.

723 Figure 1. The response of $\delta^{13}\text{C}_{\text{carbonate}}$ and $\delta^{34}\text{S}_{\text{sulfate}}$ to a 50% increase in organic carbon and
724 pyrite burial for 1 m.y. As a result of increased pyrite burial, sulfate concentrations
725 fell from 28.0 to 27.8 mM. Pre-perturbation mass and isotope compositions were
726 adopted from Kurtz et al. (2003) and approximate the Cenozoic C and S cycles at
727 steady-state.

728

729 Figure 2. Stratigraphic column and geochemical data for the March Point and Petit Jardin
730 Formations of the Port au Port Group, Newfoundland, Canada.

731

732 Figure 3. Compilation of Ediacaran-Ordovician $\delta^{13}\text{C}_{\text{carbonate}}$ (Halverson et al., 2005; Derry et
733 al., 1994; Hayes et al., 1999; Saltzman 2005) and $\delta^{34}\text{S}_{\text{sulfate}}$ (Hurtgen et al., 2002;
734 Kampschulte and Strauss, 2004; Fike et al., 2006) and $\delta^{34}\text{S}_{\text{pyrite}}$ (Canfield and Teske,
735 1996; Gorjan et al., 2000; Schöder et al., 2004; Hurtgen et al., 2006; Fike et al.,
736 2006).

737

738 Figure 4. $\delta^{34}\text{S}_{\text{sulfate}}$ response to a stepwise, 50% increase in F_{py} for 1 m.y. (from 2 to 3 m.y. and
739 represented by gray band) under varying initial sulfate concentrations (0.28 mM, $\tau =$
740 0.27 m.y.; 1.9 mM, $\tau = 1.80$ m.y.; and 2.5 mM, $\tau = 3.33$ m.y.).

741

742 Figure 5. $\delta^{34}\text{S}_{\text{sulfate}}$ response to a stepwise, 100% increase in F_{py} and 10‰ increase in $\Delta^{34}\text{S}$
743 (from 25 to 35‰) for 1 m.y. (from 2 to 3 m.y. and represented by gray band) under
744 varying initial sulfate concentrations (0.70 mM, $\tau = 0.67$ m.y.; 2.1 mM, $\tau = 2.00$ m.y.;
745 and 3.5 mM, $\tau = 3.33$ m.y.).

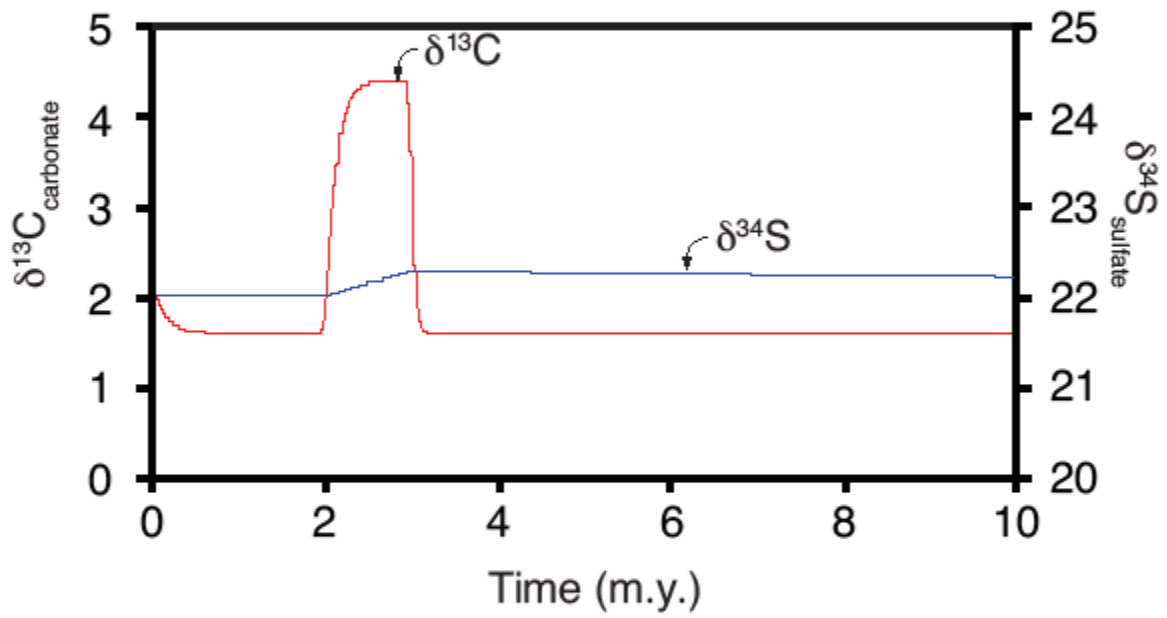


Figure 1, Hurtgen et al.

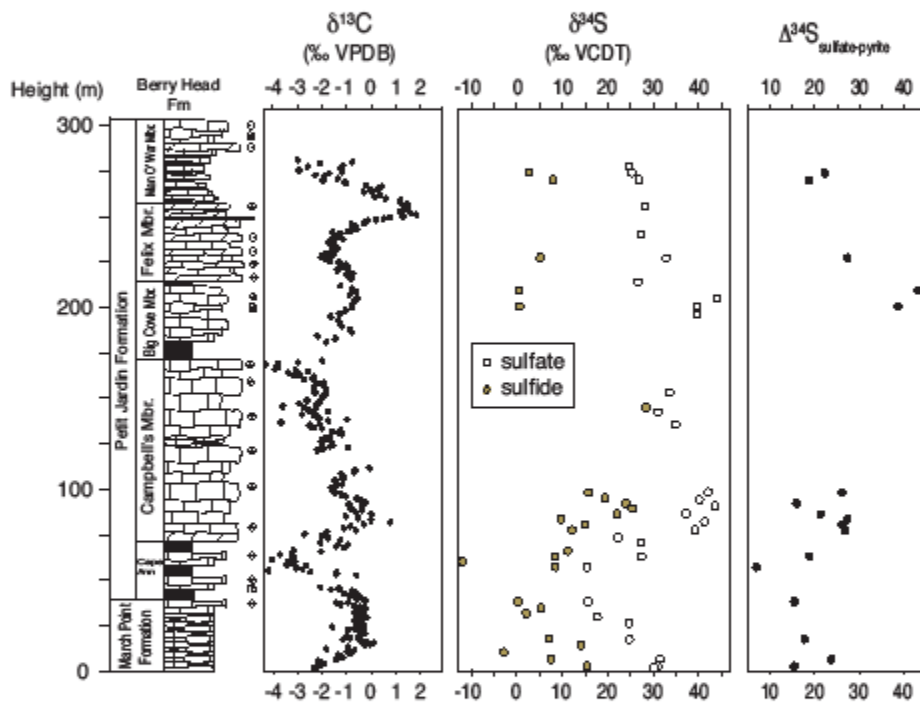


Figure 2, Hurtgen et al.

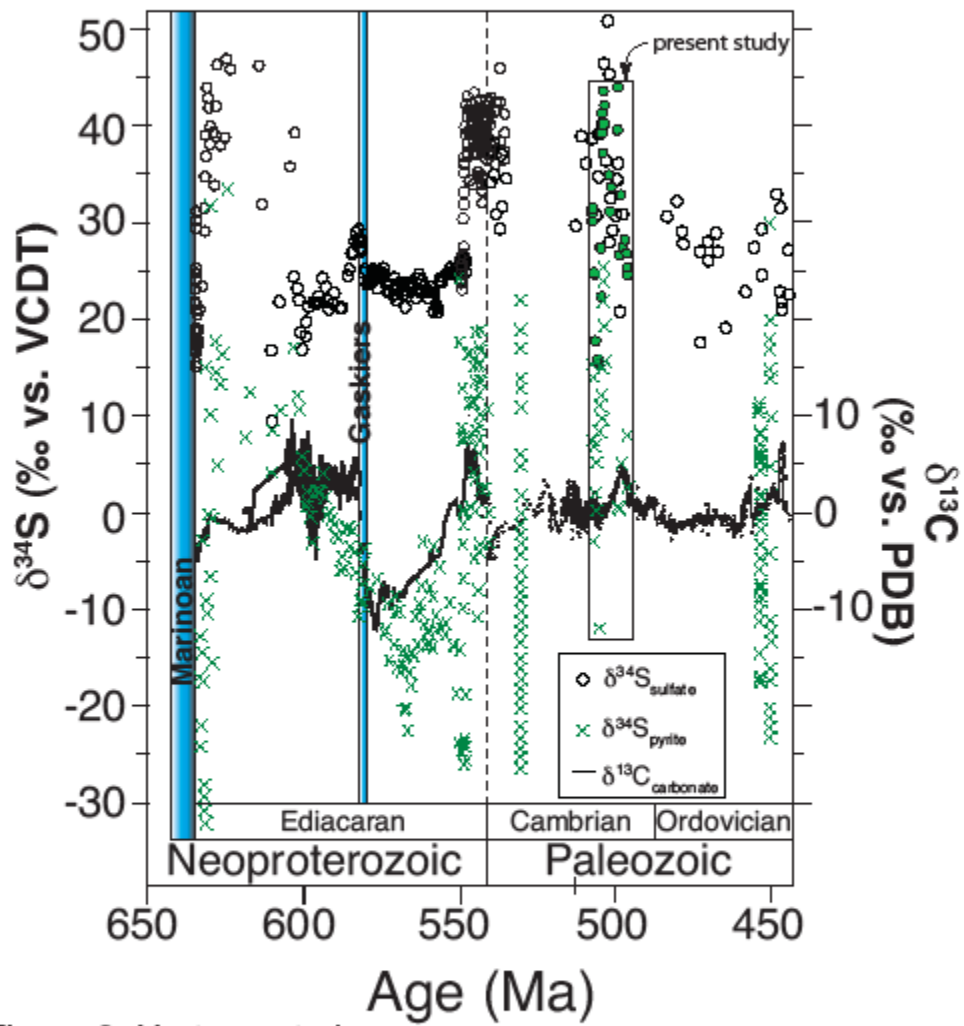


Figure 3, Hurtgen et al.

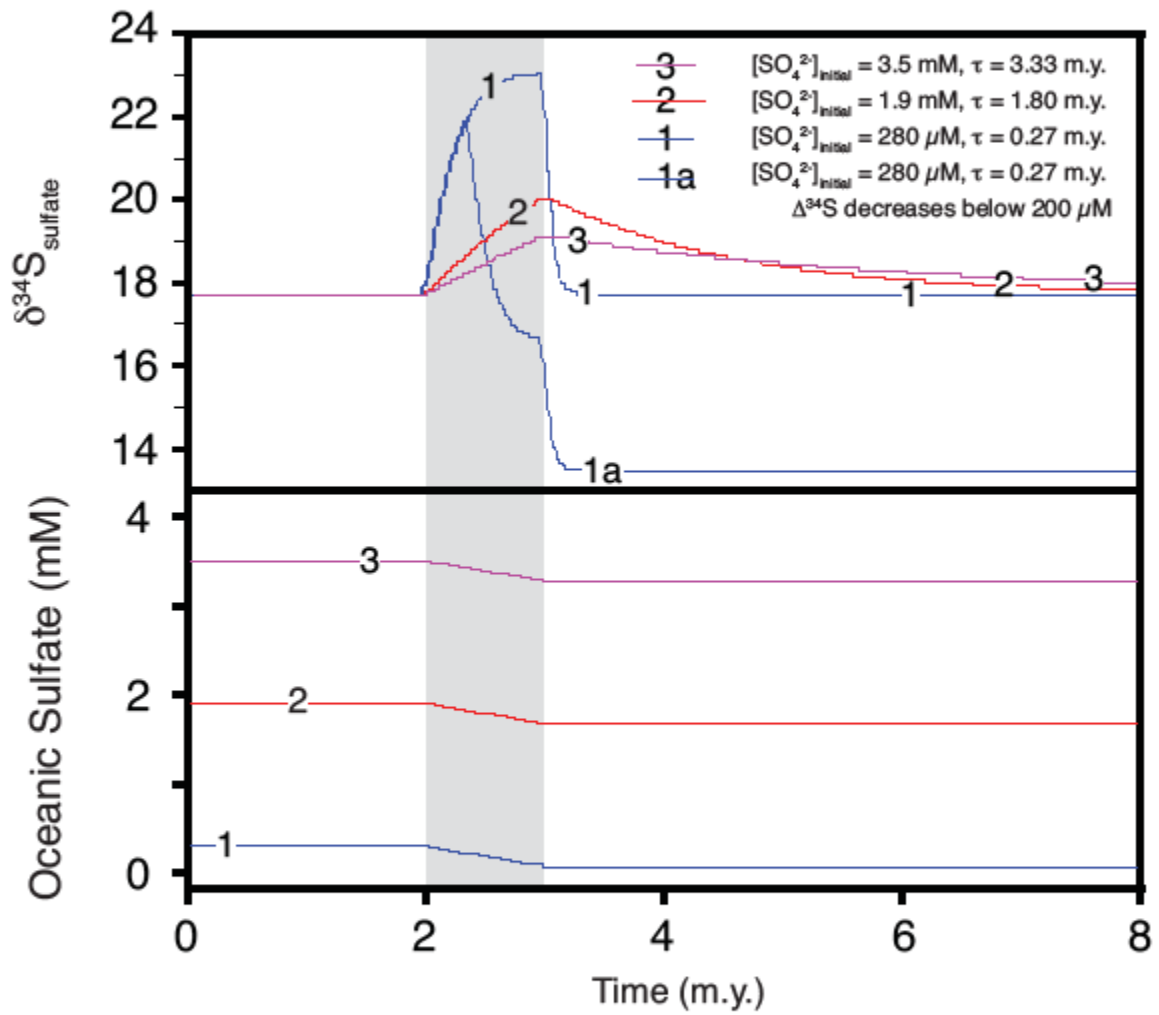


Figure 4, Hurtgen et al.

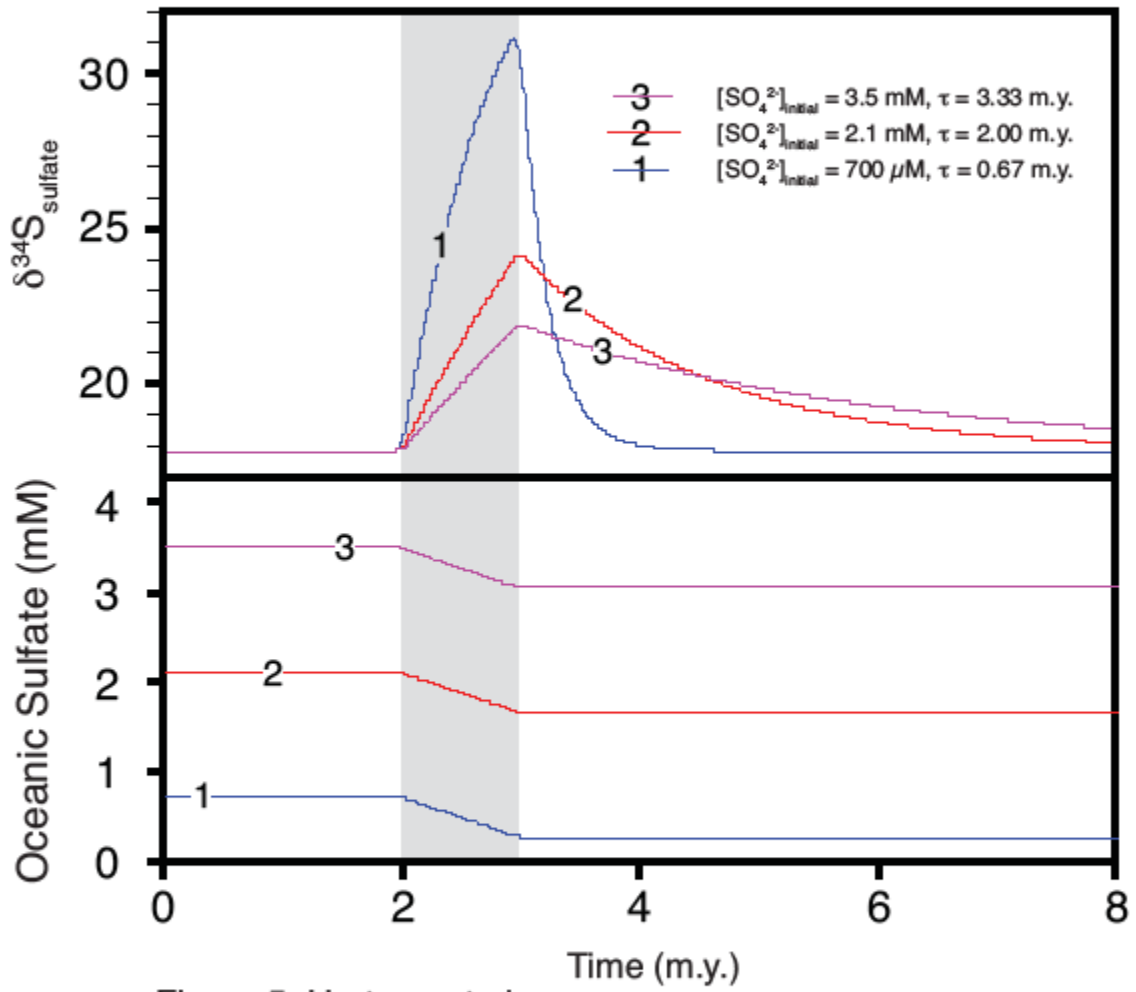


Figure 5, Hurtgen et al.